

High peak power density and low mechanical stress photonic-band-crystal diode laser array based on non-soldered packaging technology

Jing Liu (刘靖)^{1,2*}, Mingjin Wang (王明金)¹, Yufei Wang (王宇飞)^{1,2,3,4}, Xuyan Zhou (周旭彦)¹, Ting Fu (傅廷)^{1,2}, Aiyi Qi (齐爱谊)^{1,3}, Hongwei Qu (渠红伟)^{1,2,3,4}, Xiaoxu Xing (邢晓旭)^{1,2}, and Wanhua Zheng (郑婉华)^{1,2,3,4,5**}

¹Laboratory of Solid-State Optoelectronics Information Technology, Institute of Semiconductors, Chinese Academy of Sciences, Beijing 100083, China

²Center of Materials Science and Optoelectronics Engineering, University of Chinese Academy of Sciences, Beijing 100049, China

³State Key Laboratory on Integrated Optoelectronics, Institute of Semiconductors, Chinese Academy of Sciences, Beijing 100083, China

⁴College of Future Technology, University of Chinese Academy of Sciences, Beijing 101408, China

⁵School of Electronic, Electrical and Communication Engineering, University of Chinese Academy of Sciences, Beijing 100049, China

*Corresponding author: jingliu@semi.ac.cn

**Corresponding author: whzheng@semi.ac.cn

Received January 28, 2022 | Accepted April 24, 2022 | Posted Online May 24, 2022

A high peak power density and low mechanical stress photonic-band-crystal (PBC) diode laser array based on non-soldered packaging technology is demonstrated. The array consists of the PBC diode laser bars with small fast axis divergence angles. Meanwhile, we design the non-soldered array structure that realizes mechanical stacking of 10 bars in the vertical direction. In the experiment, the peak power density of the PBC array is about 1.75 times that of the conventional array when the same total power is obtained. The peak power of the non-soldered array is 292.2 W, and the “smile” effect is improved by adjusting the mechanical fixing force of the array.

Keywords: photonic-band-crystal; non-soldered packaging; low mechanical stress.

DOI: [10.3788/COL202220.071403](https://doi.org/10.3788/COL202220.071403)

1. Introduction

A high power diode laser array with advantages of high peak power, high conversion efficiency, and high reliability is widely used in many fields, such as industrial processing, communication, medicine, and beauty^[1-5]. In 2018, a multi-bar array with bar-to-bar pitch as low as 350 μm and total peak power of over 1 MW was reported by Lasertel Inc. The multi-bar array was used to pump a variety of fiber and solid-state materials^[6]. In 2021, a multi-bar array assembled over 750 kW of peak optical power within a small emission area was reported by Leonardo Electronics US, Inc.^[7].

Up to now, fast axis divergence angles of the high power diode laser array based on conventional diode laser bars are about 36° (FWHM). Therefore, the high peak power density of the diode laser array can only be achieved by external fast axis beam shaping. The peak power density of the high power diode laser array is seriously restricted by fast axis divergence angles of conventional diode lasers^[8]. In 2011, the Technical University Berlin reported that the PBC structure was added to conventional diode laser chips at 1060 nm, reducing fast axis divergence

angles^[9]. In 2021, we demonstrated high power PBC diode laser bars with about 15° (FWHM) fast axis divergence angles^[10].

With application requirements increasing, the better beam quality of the high power vertical diode laser array is required, especially the low “smile.” When the high power diode laser bar works, the positions of emitters (in a laser bar) shift in microns in the fast axis direction. The phenomenon is called the “smile” effect. Generally, the 5 μm “smile” causes two times reduction of beam quality^[11]. The “smile” seriously affects the laser beam transmission, shaping, and focusing. It is harmful to diode laser array applications in the fields of solid-state laser pumping, fiber coupling, and external cavity beam combining^[12-14]. The most important factor that provokes the “smile” phenomenon is mechanical stress. Mechanical stress is induced by mismatch of the coefficient of thermal expansion (CTE) between the materials of diode lasers and heat sinks^[15-20]. For conventional packaging of the high power diode laser array, the microchannel cooler (MCC) material is oxygen-free copper, so it must be bonding with a ductile soft solder. However, it is unavoidable that there is a mismatch of CTE between materials of the laser bar and MCC^[21]. In addition, when indium solder works under

a high temperature for a long time, fatigue failure accelerates degradation of diode laser bars.

In this paper, a high peak power density and low mechanical stress PBC diode laser array based on non-soldered packaging technology is demonstrated. The PBC diode laser array consists of the bars with small fast axis divergence angles. PBC structures are added to the bars, so fast axis divergence angles of bars are reduced to about 15° (FWHM). Through simulation of ray tracing, the peak power density of the PBC array is 1.9 times that of the conventional array in free transmission. In this case, even if adding an external beam shaping system or reducing bar-to-bar pitch, the peak power density of the PBC array still has great advantages over the conventional array. We design the non-soldered array structure that realizes mechanical stacking of 10 bars in the vertical direction. In order to ensure good heat dissipation and electrical connection, InSn solder foils are placed to P and N sides of the bar. InSn solder with better ductility can fill the gap caused by contact between solids. A small amount of Sn doped with indium could reduce degeneration of laser bars greatly. Multiphysics simulation results show that stress of the PBC diode laser bar with indium soldered is about 18.6 times the stress of the PBC diode laser bar with non-soldered.

In the experiment, the PBC diode laser array with two non-soldered bars is demonstrated. The peak power density of the array is about 1.75 times that of the conventional diode laser array when the same total power is obtained. Peak power of the PBC diode laser array with non-soldered is 292.2 W, and the “smile” effect is improved by adjusting mechanical fixing force.

2. Structure Designs and Simulation Results

A single MCC laser packaging structure with the non-soldered is designed, as shown in Fig. 1. The L-shaped elastic insulating foil is placed on the MCC. It is used to insulate the anode and cathode of the bar and to locate bar and InSn foil. One piece of InSn foil with a size of $10\text{ mm} \times 2\text{ mm} \times 0.03\text{ mm}$ is placed on the top surface of the MCC, ensuring that the P side of the laser bar is connected to the MCC tightly. Another piece of InSn foil (the same size as the first one) is placed on the bar, ensuring that the N side of the bar is tightly connected to the cathode. The last layer is the cathode whose thickness is about $50\text{ }\mu\text{m}$.

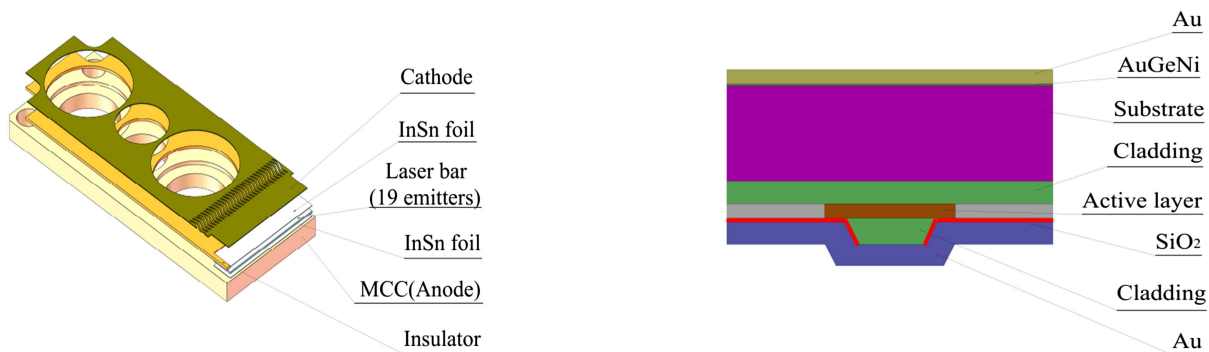


Fig. 1. Schematic of a single MCC diode laser.

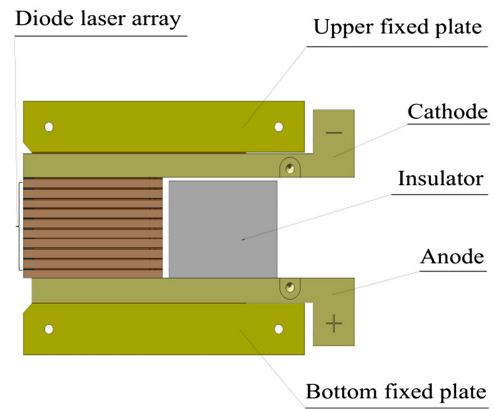


Fig. 2. Schematic of the vertical diode laser array.

Ten pieces of MCC lasers are placed in a vertical stack by mechanical fixing, as shown in Fig. 2. The block of the rear position is designed to control the height of the entire stack accurately, ensuring that 10 bars avoid bearing a large mechanical force.

The size of the bar is $10\text{ mm} \times 2\text{ mm} \times 0.135\text{ mm}$ with a total of 19 emitters. Each emitter width is $200\text{ }\mu\text{m}$, and the pitch is $500\text{ }\mu\text{m}$. P and N sides of the laser bar are covered with micron-level Au layer. The emitter layer structure is shown in Fig. 3. From top to bottom, the N-side metal layer, GaAs substrate, P cladding layer, active area, N cladding layer, and P-side metal layer are arranged continuously. Table 1 shows the parameters of the PBC and conventional laser bar.

The simulations of ray tracing are shown in Figs. 4(a) and 4(b). In free transmission, the peak irradiance of the PBC diode laser array is $1.34 \times 10^4\text{ W/cm}^2$, and the peak irradiance of the conventional diode laser array is $7.01 \times 10^3\text{ W/cm}^2$. The peak irradiance of the PBC diode laser array is about 1.9 times that of the conventional diode laser array, so it is easier to obtain high peak power density with the PBC diode laser array.

Taking into account the structural symmetry of the monolithic laser bar, we only establish the unilateral model of one laser bar. The bar is meshed and solved through multiphysics simulation, as shown in Fig. 5. Stress, displacement, and temperature distribution of the PBC laser bar with non-soldered and indium

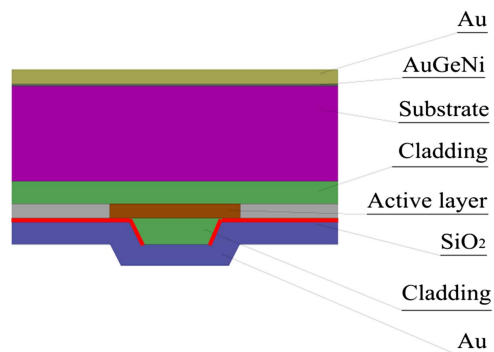


Fig. 3. Schematic of a single PBC laser emitter.

Table 1. Parameters of PBC and Conventional Laser Bar.

Parameters	PBC Laser Diode	Conventional Diode Laser
Fast axis divergence (FWHM)	15°	36°
Slow axis divergence (FWHM)	7°	7°
Emitter width in the slow axis	200 μm	200 μm
Number of emitters	19	19
Emitter pitch	500 μm	500 μm

soldered are simulated. For the array with indium soldered, the residual stress and deformation during annealing are applied to the model as initial conditions. The working temperature and fixed constraints as boundary conditions are applied to the solution. The bonding temperature is 240°C. The output peak

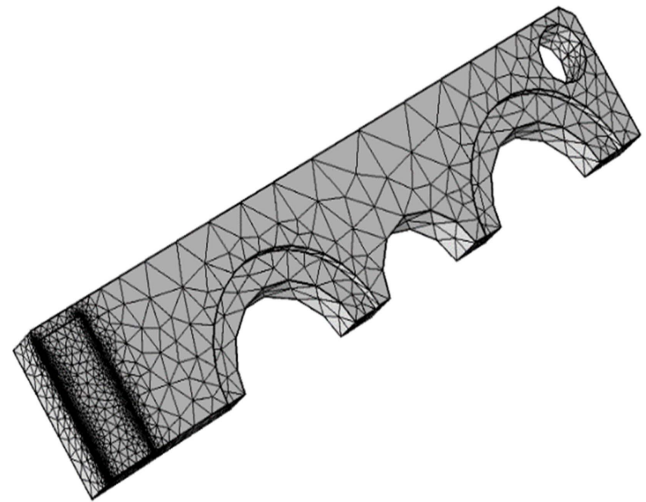


Fig. 5. Simulation model of the PBC laser bar.

power is 100 W. The duty cycle is 10%, and the electro-optical conversion efficiency is set to 50%. Average thermal power of 10 W is generated when the laser bar is working. Table 2 shows the parameters of material performance.

For the PBC laser bar with indium soldered, the CTEs of the heat sink material and the bar material (GaAs) are mismatched during annealing. It generates stress on the bar, and the peak stress is 3.34×10^9 N/cm². For the PBC laser bar with non-soldered, InSn foil is used as a gasket to fill the hard contact gap between the bar and the heat sink. The peak stress of the PBC laser bar with non-soldered is only 1.8×10^8 N/cm². The stress of the PBC laser bar with indium soldered is 18.6 times that of the PBC laser bar with non-soldered, as shown in Figs. 6(a) and 6(b). The low stress could improve the “smile” effect and beam quality.

Because of mutual constraint between the bar and MCC with indium soldered, the deformation of the bar with indium soldered is smaller than that of the bar with non-soldered. The peak deformation of the bar with indium soldered is 0.5 μm and the peak deformation of the bar with non-soldered is 0.8 μm, as shown in Figs. 7(a) and 7(b). Peak deformations of two bars are on the scale of microns, so there is little influence on the whole packaging.

Figures 8(a) and 8(b) show the heat distribution of the two bars. The maximum junction temperatures are both 46.6°C, indicating that the laser bars with indium soldered and non-soldered could work stably when they are well connected to the heat sinks.

3. Experiments and Discussions

The light spots of the conventional diode laser bar and PBC diode laser bar in the free transmission are measured by CCD, as shown in Figs. 9(a) and 9(b). The CCD sampling aperture is set, ensuring that their total number of photons can be equal in quantity. In this case, the peak photon number of the

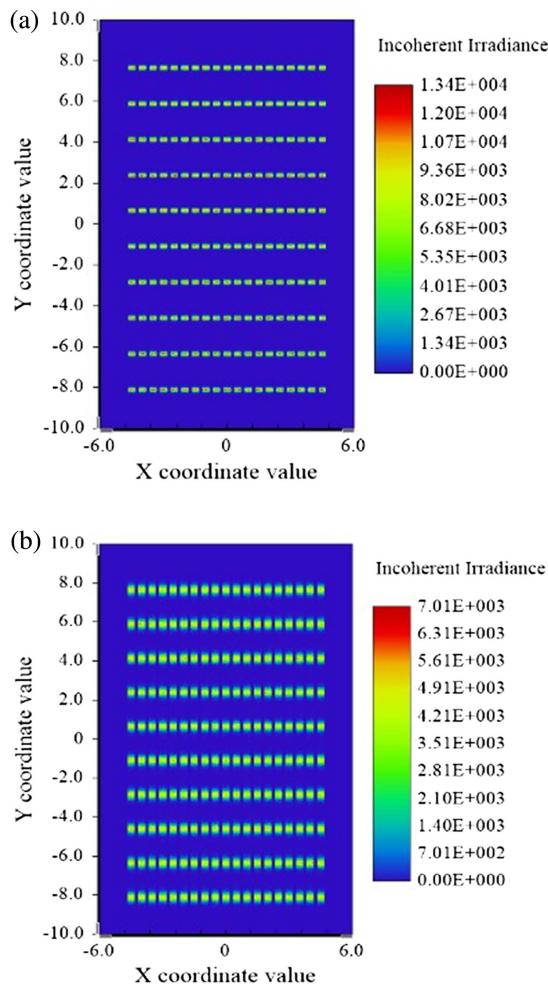


Fig. 4. Far-field incoherent irradiance distribution of the two diode laser arrays. (a) Irradiance distribution of the PBC diode laser array. (b) Irradiance distribution of the conventional diode laser array.

Table 2. Parameters of Material Performance.

Material	Density ($\text{kg} \cdot \text{m}^{-3}$)	CTE (10^{-6}K^{-1})	Thermal Conductivity ($\text{W} \cdot \text{m}^{-1} \cdot \text{K}^{-1}$)	Poisson's Ratio	Heat Capacity ($\text{J} \cdot \text{kg}^{-1} \cdot \text{K}^{-1}$)	Young's Modulus (Pa)
Cu	8900	16.5	398	0.36	395	1.3×10^{11}
GaAs	5330	6.4	44	0.30	325	7.5×10^9
In	7310	33	81.6	0.45	230	1.1×10^{10}
InSn	7300	20	34	0.45	230	1.6×10^{10}

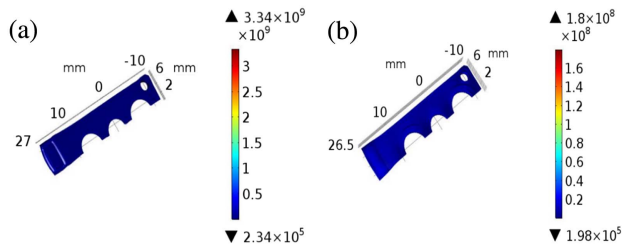


Fig. 6. Stress distribution of the two PBC diode laser bars. (a) Stress distribution of the bar with indium soldered. (b) Stress distribution of the bar with non-soldered.

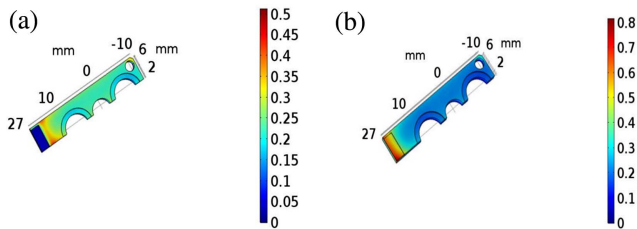


Fig. 7. Deformation distribution of the two PBC diode laser bars. (a) Deformation distribution of the bar with indium soldered. (b) Deformation distribution of the bar with non-soldered.

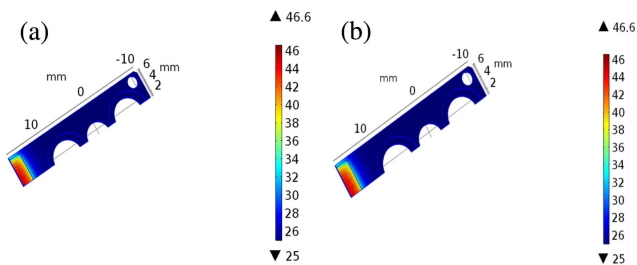


Fig. 8. Temperature distribution of the two PBC diode laser bars. (a) Temperature distribution of the bar with indium soldered. (b) Temperature distribution of the bar with non-soldered.

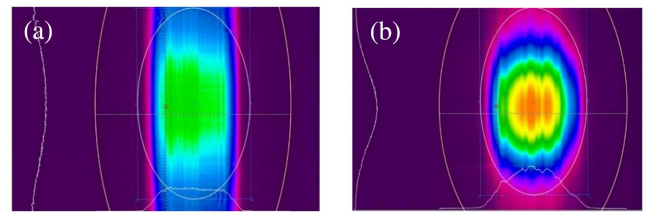


Fig. 9. Light spots in free transmission of the two diode laser bars. (a) Light spot of the conventional bar. (b) Light spot of the PBC bar.

PBC laser bar is about 1.75 times that of the conventional laser bar. It can be concluded that the peak power density of the PBC diode laser bar is higher than that of the conventional diode laser bar.

According to the above structure design, the two PBC laser bars are placed in a vertical stack by mechanical fixing, as shown in Fig. 10(a). The cavity surface is observed under the microscope, and P and N sides of the bars are in good connection with the anodes and cathodes, as shown in Fig. 10(b). Power-current-voltage (PIV) relationship and “smile” are tested.

The PBC laser arrays with indium soldered and non-soldered are measured, respectively, under the same working conditions. The pulse width is 100 μs , repetition frequency is 100 Hz, and duty cycle is 1%. As shown Figs. 11(a) and 11(b), when currents are less than 130 A, the peak power and slope efficiency of the array with indium soldered are better than those of the array with non-soldered. But, above 170 A, the peak power and slope efficiency of the array with non-soldered are significantly

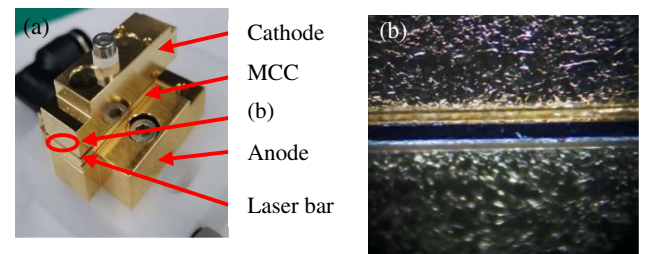


Fig. 10. (a) PBC diode laser array with two non-soldered bars. (b) P and N sides contact.

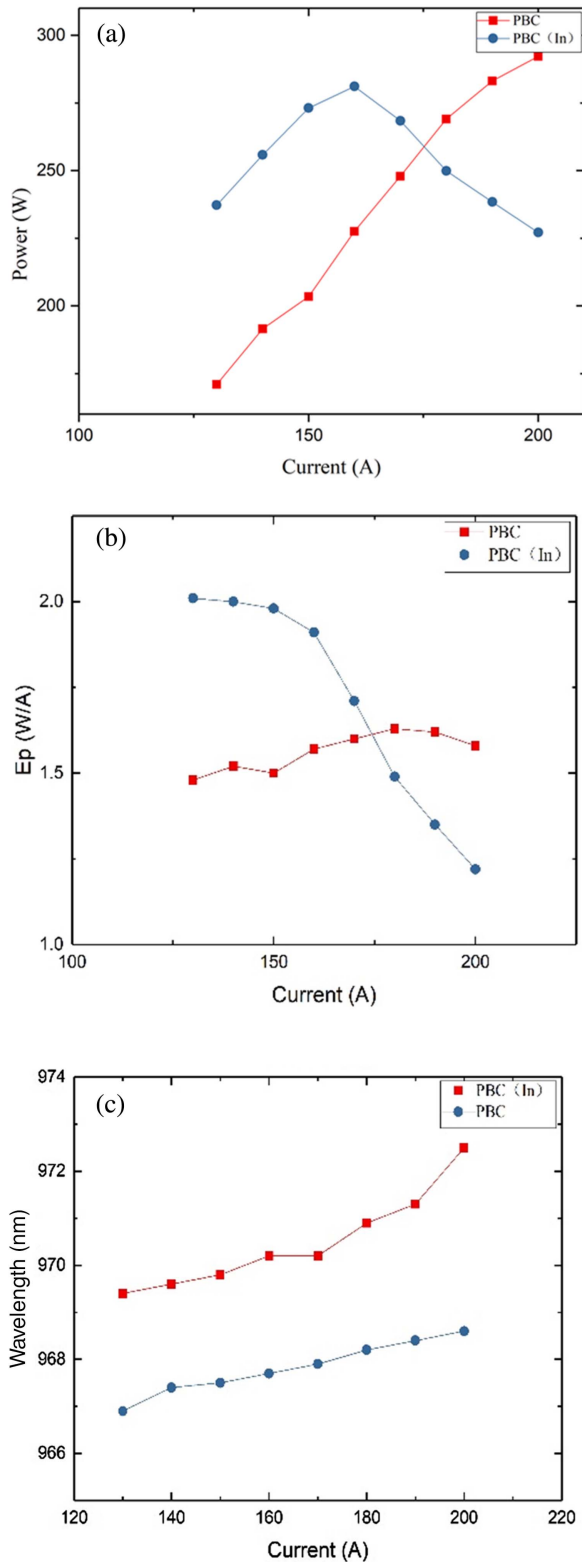


Fig. 11. (a) Power, (b) slope efficiency, and (c) wavelength of the PBC diode laser arrays with non-soldered and indium soldered.

superior. Peak power of the array with non-soldered is 292.2 W at 200 A, while that of the array with indium soldered is 227.1 W. The thermal resistance with indium soldered packaging is

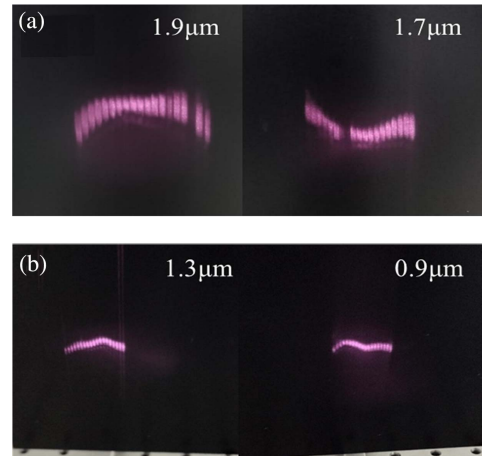


Fig. 12. "Smile" of the PBC diode laser array with non-soldered. (a) The "smile." (b) The optimized "smile."

smaller than that with non-soldered packaging. At low current, waste heat inside laser bar is small, and the temperature of the laser bar active area is low. Therefore, the stress has no obvious effect on the performance of the laser bar, and output power of the laser bar with indium soldered packaging is higher. At high current, the temperature of the laser bar active area is high, and the stress has a significant impact on the performance of the laser bar. The laser bar with non-soldered packaging has less stress, so the output is higher.

With increasing current, the wavelength red shifting is basically the same, as shown in Fig. 11(c). Only at 200 A, the peak power of the indium soldered array falls largely, resulting in the thermal effect increasing and wavelength red shifting severely.

In the "smile" testing experiment of the array with non-soldered, the mechanical fixing force is reduced, and the "smile" effect is improved obviously, as shown in Figs. 12(a) and 12(b). It can be seen that the mechanical fixing force has a great influence on the "smile" effect for the array with non-soldered.

4. Conclusion

In summary, the PBC laser bars with low fast divergence angles are adopted in the PBC array. A single MCC diode laser bar structure based on non-soldered packaging technology is designed. The PBC diode laser array consists of ten bars with non-soldered. They are arranged in a vertical stack by mechanical fixing force.

Simulation results show that peak power density of the PBC diode laser array is about 1.9 times that of the conventional diode laser array under the same working conditions. Mechanical stress and heat distribution of the PBC diode laser bar with non-soldered and indium soldered are simulated. The results show that the highest junction temperatures of two bars are 46.6°C, but the mechanical stress of the bar with indium soldered is 18.6 times that of the bar with non-soldered. In the experiment, the PBC diode laser array with two non-soldered bars is carried out. The light spots of the PBC diode laser bar

and conventional diode laser bar in the free transmission are measured by CCD, and the peak power density of the PBC laser bar is about 1.75 times that of the conventional laser bar. The peak power of the array with non-soldered is 292.2 W at 200 A, while that of the array with indium soldered is only 227.1 W. The “smile” effect of the PBC laser bars with non-soldered is improved obviously when the mechanical fixing force is reduced. “Smile” values decrease from 1.9 μm and 1.7 μm to 1.3 μm and 0.9 μm . It can be seen that low mechanical stress, high beam quality, and high power density can be achieved through the PBC diode laser array with non-soldered.

Future works will include increasing peak power of the PBC array with non-soldered and optimizing the mechanical fixing force to improve the “smile” effect.

Acknowledgement

This work was supported in part by the National Key R&D Program of China (No. 2021YFA1400604) and the National Natural Science Foundation of China (Nos. 91850206 and 62075213).

References

1. Y. Jia, Y. Wang, X. Zhou, L. Xu, P. Ma, J. Chen, H. Qu, and W. Zheng, “Narrow vertical beam divergence angle for display applications of 645 nm lasers,” *Chin. Opt. Lett.* **19**, 101401 (2021).
2. J. Hecht, “Short history of laser development,” *Opt. Eng.* **49**, 091002 (2010).
3. V. Shchukin, N. Ledentsov, K. Posilovic, V. Kalosha, T. Kettler, D. Seidlitz, M. Winterfeldt, and D. Bimberg, “Tilted wave lasers: a way to high brightness sources of light,” *IEEE J. Quantum Electron.* **47**, 1014 (2011).
4. S. Hengesbach, R. Poprawe, D. Hoffmann, M. Traub, T. Schwarz, C. Holly, F. Eibl, A. Weisheit, S. Vogt, S. Britten, M. Ungers, U. Thombsen, C. Engelmann, V. Mamuschkin, and P. Lott, “Brightness and average power as driver for advancements in diode lasers and their applications,” *Proc. SPIE* **9348**, 93480B (2015).
5. W. Fassbender, H. Kissel, J. Lotz, T. Koenning, S. Patterson, and J. Biesenbach, “Reliable QCW diode laser arrays for operation with high duty cycles,” *Proc. SPIE* **10085**, 1008509 (2017).
6. D. Crawford, P. Thiagarajan, J. Goings, B. Caliva, S. Smith, and R. Walker, “Advancements of ultra-high peak power laser diode arrays,” *Proc. SPIE* **10514**, 105140H (2018).
7. L. Woods, M. Crowley, P. Thiagarajan, E. Ruben, J. Goings, T. Hosoda, M. Rowe, B. Liu, B. Caliva, and N. Crapo, “Ultra-high peak power laser diode arrays with 1 kA-class low-SWaP drive electronics,” *Proc. SPIE* **11667**, 1166703 (2021).
8. W. Fassbender, J. Lotz, H. Kissel, and J. Biesenbach, “Novel packaging for CW and QCW diode laser modules for operation with high power and duty cycles,” *Proc. SPIE* **10513**, 105130M (2018).
9. V. P. Kalosha, K. Posilovic, T. Kettler, V. A. Shchukin, N. N. Ledentsov, and D. Bimberg, “Simulations of the optical properties of broad-area edge-emitting semiconductor lasers at 1060 nm based on the PBC laser concept,” *Semicond. Sci. Technol.* **26**, 075014 (2011).
10. Z. Chen, A. Qi, X. Zhou, H. Qu, J. Chen, Y. Jia, and W. Zheng, “High power and narrow vertical divergence laser diodes with photonic crystal structure,” *IEEE Photonics Technol. Lett.* **33**, 399 (2021).
11. N. U. Wetter, “Three-fold effective brightness increase of laser diode bar emission by assessment and correction of diode array curvature,” *Optics & Laser Technology* **33**, 181 (2001).
12. Z. Wu, S. You, Q. Du, and Y. Huang, “Influence of smile effect on beam properties of spectrally combined beams based on diode laser stacks,” *Opt. Commun.* **471**, 126031 (2020).
13. F. Sun, Y. Zhao, S. Shu, G. Hou, H. Lu, X. Zhang, L. Wang, S. Tian, C. Tong, and L. Wang, “High beam quality broad-area diode lasers by spectral beam combining with double filters,” *Chin. Opt. Lett.* **17**, 011401 (2019).
14. T. Wang, L. Wang, S. Shu, S. Tian, Z. Zhao, C. Tong, and L. Wang, “Suppression of far-field blooming in high-power,” *Chin. Opt. Lett.* **15**, 071404 (2017).
15. Z. Nie, Y. Lu, T. Chen, P. Zhang, D. Wu, M. Wang, L. Xiong, X. Li, Z. Wang, and X. Liu, “Thermomechanical behavior of conduction-cooled high-power diode laser arrays,” *IEEE Trans. Compon. Packag. Manuf. Technol.* **8**, 818 (2018).
16. G. Jia, S. Yao, X. Luo, J. Cheng, and Z. Wang, “The smile effect reduction of diode laser bar by bare bar curve control,” *Proc. SPIE* **10085**, 100850D (2017).
17. D. Lisak, D. T. Cassidy, and A. H. Moore, “Bonding stress and reliability of high power GaAs-based lasers,” *IEEE Trans. Compon. Packag. Technol.* **24**, 92 (2001).
18. M. L. Biermann, S. Duran, K. Peterson, A. Gerhardt, J. W. Tomm, A. Bercha, and W. Trzeciakowski, “Spectroscopic method of strain analysis in semiconductor quantum-well devices,” *J. Appl. Phys.* **96**, 4056 (2004).
19. M. A. Fritz and D. T. Cassidy, “Extraction of bonding strain data in diode lasers from polarization-resolved photoluminescence measurements,” *Microelectronics Reliability* **44**, 787 (2004).
20. C. Scholz, K. Boucke, and R. Poprawe, “Mechanical stress-reducing heat sinks for high-power diode lasers,” *Proc. SPIE* **5336**, 175 (2004).
21. M. Leers, C. Scholz, K. Boucke, and R. Poprawe, “Expansion-matched passively cooled heatsinks with low thermal resistance for high-power diode laser bars,” *Proc. SPIE* **6104**, 610403 (2006).